Anisotropic electrical conductivity and low-temperature phase transitions of the solid electrolyte $Ag_{26}I_{18}W_4O_{16}$

S. Geller, S. A. Wilber, G. F. Ruse,* J. R. Akridge,† and A. Turkovič‡
Department of Electrical Engineering, University of Colorado, Boulder, Colorado 80309
(Received 27 August 1979)

Results of measurements of electrical conductivity of single crystals of $Ag_{26}I_{18}W_4O_{16}$ in the temperature range 473–175 K show the existence of two first-order transitions at 246 and 197 K; the phases are labeled α, β, γ in order of decreasing temperature. *Within experimental error*, the principal conductivity axes of the α phase are $\vec{a}$, $\vec{b}$, and $\vec{c}^*$ over its temperature range of existence. At 25°C, the principal conductivities are 0.120, 0.085, and 0.083 $\Omega^{-1}\text{cm}^{-1}$, respectively, and the average conductivity, 0.097 $\Omega^{-1}\text{cm}^{-1}$, is 1.6 times the best value obtained from conductivity measurements on polycrystalline material. It is shown that the $\log_{10}(\sigma T)$ vs T^{-1} data for the α phase imply that the activation enthalpies of motion are temperature dependent. It is also likely that very few Ag^+ ions are thermally excited from the immobile to the mobile category. The magnitudes of the activation enthalpies of motion of the β and γ phases appear to be constant, and suggest that there is greater (possibly complete) order in the γ than in the β phase and greater order in the β than in the α phase.

INTRODUCTION

Crystals of $Ag_{26}I_{18}W_4O_{16}$ belong to space group $C2$ (C_2^3), with $a = 16.76 \pm 0.03$, $b = 15.52 \pm 0.03$, $c = 11.81 \pm 0.02$ Å, $\beta = 103.9° \pm 0.3°$. The unit cell contains 2 $Ag_{26}I_{18}W_4O_{16}$, i.e., one $Ag_{26}I_{18}W_4O_{16}$ per *primitive* unit cell. The crystal structure, including the distribution of Ag^+ ions at room temperature, has been determined.[1] The symmetry is very low; the crystals belong to the lowest symmetry monoclinic point group, namely 2 (C_2).

Measurements of directional conductivity have been made on very few solid electrolytes: Na β-alumina,[2] $(C_5H_5NH)Ag_5I_6$, and $(C_5H_5NH)_5Ag_{18}I_{23}$ [$(C_5H_5NH)^+$ is pyridinium].[3] All these have hexagonal symmetry, high, relative to that of $Ag_{26}I_{18}W_4O_{16}$; they require measurements in only two directions (along $\vec{c}$ and perpendicular to $\vec{c}$) for the determination of the conductivity tensor components.

The solid electrolyte $Ag_{26}I_{18}W_4O_{16}$ appeared to be an excellent candidate for investigation of the directional conductivity of a low-symmetry crystal. There appeared to be a high probability that crystals of it could be grown from the melt by the Czochralski technique. The phase diagram reported[4] for the "Ag_2WO_4"-AgI system indicated that the solid electrolyte melts incongruently; this had been corroborated by us in our earliest attempts to obtain crystals for the crystal-structure determination. The incongruent melting presented difficulty in the growth of the crystals. It is intended to give details on the crystal growth elsewhere; suffice it to say here that although the crystal-growth problem was a formidable one, crystals of size and quality sufficient for the conductivity measurements were obtained. As far as we know, nobody else has succeeded in growing such crystals.

The results of the measurements show unequivocally two first-order transition at 197 and 246 K. The anisotropy of the conductivity is not as dramatic as it is for the hexagonal crystals mentioned earlier, but this was to be expected from the crystal structures. At 25°C, the average conductivity obtained from the crystals is 1.6 times higher than the highest value obtained for single-phase polycrystalline material.[1]

EXPERIMENTAL

Crystals had been grown along the $\vec{a}$, $\vec{b}$, and $\vec{c}$ directions, and it was necessary to cut $\vec{c}^*$ directed specimens from these. Cutting was done with a wire saw. Glycerine was used as a lubricant; it was important not to allow water to be absorbed by it. The abrasive was 5-μm alumina. Geoscience's low-melting (40°C) Loc-wax was used to hold the crystal firmly to a thick glass slide during cutting. It was necessary to cut the crystals very slowly to avoid cracking and stepped surfaces. Warm trichloroethylene was used to dissolve the wax away from the crystal.

Alignment was carried out by photographing pieces, sometimes wedge-shaped, with a Buerger precession x-ray diffraction camera. These pieces had been indexed on the bulk crystals making it possible then to cut the required pieces from the bulk crystals.

The "electroding" of the crystals was quite difficult largely because of their brittleness. After much experimentation with silver epoxy and silver

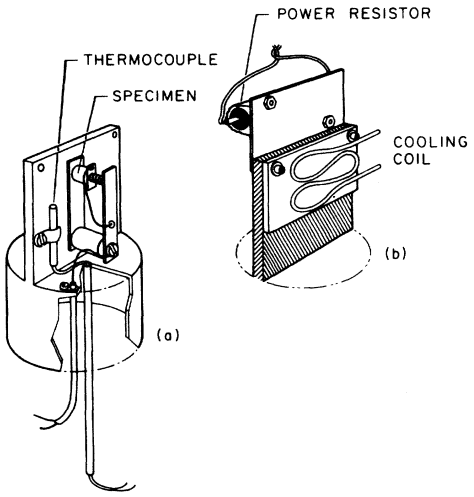

FIG. 1. (a) Device used for conductivity measurements. For high-temperature measurements, it is placed into a closed-end brass cylinder fitted into a small furnace. (b) Cooling coil and power resistor attached for low-temperature measurements.

disks, a technique was developed by which a layer of silver powder was made to adhere to the appropriate surfaces.

First the ends of the crystal were lightly smoothed on a clean, flat sheet of No. 600 carbide paper. Then a small amount of one-micron silver (99.99%) powder was placed on a section of the carbide paper. The crystal ends were lightly rubbed over the silver powder until a thin coating adhered to the surface. (Adhesion resulted from surface abrasion.) The ends were then polished on No. 4/0 emery paper covered with silver powder until a light, metallic sheen developed over the entire end surfaces. The crystal was subsequently placed between silver disks under spring tension (Fig. 1). The technique, although tedious, results in electrodes with good electrical and mechanical properties, stable with time and over the temperature range of measurement.

For the conductivity measurements, the equipment used is shown in Fig. 1(a). For heating, the device is placed into a brass cylinder, with $\frac{1}{8}$-in. walls, closed at one end and fitted into a small resistance furnace, specially made to enclose the cylinder. The device makes contact at all outer walls with the inside of the brass cylinder. The arrangement ensures temperature uniformity. Input power is furnished through a variable autotransformer. Temperatures are measured with a copper-constantan thermocouple and a potentiometer.

For the low-temperature measurements, nitrogen is passed through a coil surrounded by liquid nitrogen, then through a coil [see Fig. 1(b)] solidly connected to the brass plate of Fig. 1(a). Also connected to the plate is a 40-ohm power resistor. The whole assembly is then insulated from the atmosphere by fitted, thick styrofoam blocks. An Oxford Instruments DTC2 controller is used; it supplies power to the resistor when required to bring the specimen to the preset temperature. The nitrogen flow is manually controlled.

The conductivity measurements were made with the vector-impedance meter briefly described elsewhere.[5] The frequency range of the instrument has been expanded to 10^{-1} Hz to 650 kHz; originally it was 0.5 Hz to 250 kHz. This instrument enables one to measure the impedance or admittance[6] and/or to change the frequency so as to make the (capacitive) reactance negligible with respect to the resistance. For the results shown in Figs. 2 and 3, giving σT vs T^{-1}, the frequency was kept as low as possible but sufficiently high to give negligible reactance.

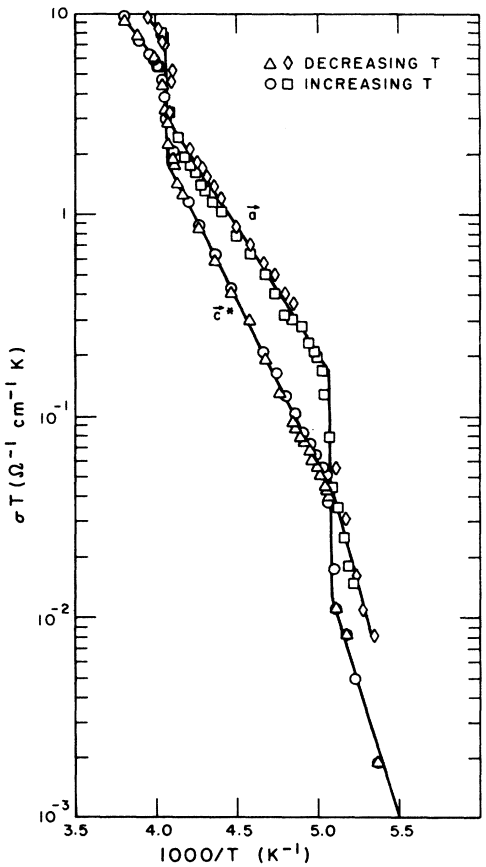

FIG. 2. Plots of $\log_{10}$ of the conductivity multiplied by temperature vs reciprocal temperature in low-temperature range for $\vec{a}$- and $\vec{c}^*$-directed crystals with small length to area ratios. Points taken with decreasing and increasing temperature are distinguished.

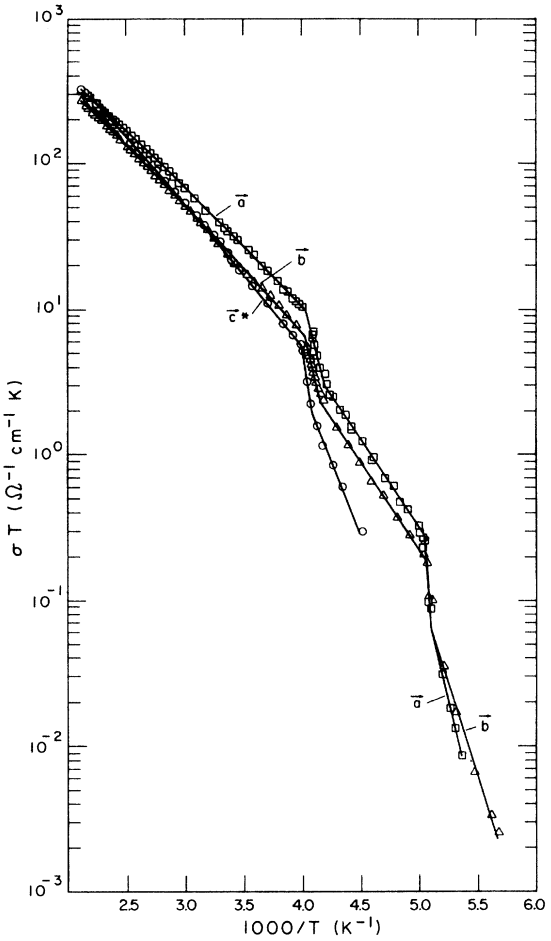

FIG. 3. Plots of $\log_{10}$ of the conductivity multiplied by temperature vs reciprocal temperature for crystals with large length to area ratios. (For the sake of clarity, points taken with decreasing and increasing temperature are not distinguished.)

CONDUCTIVITY TENSOR

The electrical conductivity tensor of a monoclinic crystal contains a minimum of four components. That is to say, a minimum of four components is required to find the principal axes. One principal axis is along the twofold axis, conventionally taken as the b axis. The other principal axes lie in the monoclinic (010) plane. One should know the angles that the principal axes make with the monoclinic axes; this is equivalent to the fourth component of the tensor.

It is most convenient to make the conductivity measurements along two known perpendicular directions in the monoclinic plane, and any third known direction in that plane, and, of course, along the b axis. From the results of the measurements along directions in the monoclinic plane, one can obtain the required tensor components in the plane.

The directions in which conductivity was measured are $\vec{a}$, $\vec{b}$, $\vec{c}^*$, $\vec{c}$, where $\vec{c}^*$ is the reciprocal-lattice vector given by $(\vec{a}\times\vec{b})/(\vec{a}\cdot\vec{b}\times\vec{c})$ and is perpendicular to both $\vec{a}$ and $\vec{b}$. Thus σ_{11}, σ_{22}, σ_{33} are taken as the electrical conductivities along $\vec{a}$ ($\| x_1$), $\vec{b}$ ($\| x_2$), and $\vec{c}^*$($\| x_3$). To find σ_{13}, the relation[7]

$$\sigma_{\vec{c}} = \sum_{i,j=1}^{3} \sigma_{ij} l_i l_j \tag{1}$$

is used, where $\sigma_{\vec{c}}$ is the conductivity along c and l_i, l_j are direction cosines of $\sigma_{\vec{c}}$ with respect to the axis x_i or x_j, $i,j=1,2,3$. Because $l_2=0$, (1) contains only terms with $i,j=1,3$. The electrical conductivity tensor is symmetric, i.e., $\sigma_{ij}=\sigma_{ji}$. Thus

$$\sigma_{13} = (\sigma_{\vec{c}} - \sigma_{11} l_1^2 - \sigma_{33} l_3^2)/2 l_1 l_3 . \tag{2}$$

At room temperature, for $Ag_{26}I_{18}W_4O_{16}$, $l_1 = \cos 103.9°$ and $l_3 = \cos 13.9°$.

One can hope that the β angle does not change significantly with change in temperature. Buerger precession photographs of a crystal oriented with the b axis parallel to the x-ray beam were taken at 110° and 150°C. The β angles at these temperatures are 104.3° and 104.8° (±0.3°), respectively. These changes do not affect the results of the conductivity measurements significantly.

The principal conductivites are the eigenvalues of the matrix σ_{ij}. Because of the initial choice of axes, one of the eigenvalues is $\sigma_{22}\equiv\sigma_2$ and the others are

$$\left.\begin{matrix}\sigma_1\\ \sigma_3\end{matrix}\right\} = \frac{\sigma_{11}+\sigma_{33}}{2} \pm \left[\tfrac{1}{4}(\sigma_{11}-\sigma_{33})^2 + \sigma_{13}^2\right]^{1/2}, \tag{3}$$

where $\sigma_{11} > \sigma_{33}$. The angle θ that the principal axes make with the old axes is given by[7]

$$\theta = \tfrac{1}{2}\tan^{-1}[2\sigma_{13}/(\sigma_{11}-\sigma_{33})] . \tag{4}$$

It should be particularly noted that θ can be quite sensitive to errors in σ_{13} which is derived from (2).

RESULTS

It will be demonstrated later that the measurements showed the occurrence of two first-order transitions at 197 and 246 K. For ease of discussion, the three phases will now be labeled α,β,γ in order of decreasing temperature. The α phase is the monoclinic phase, the crystal structure of which is known[1]; nothing is yet known about the crystal structures of the β and γ phases.

Two sets of measurements were made on different crystals in the temperature range 473–175 K.

TABLE I. Lengths, length to area ratios, parabola parameter values, and activation enthalpies of motion at 298 and 473 K.

Crystal direction →	$\vec{a}$	$\vec{b}$	$\vec{c}^*$	$\vec{c}$
l (cm)	0.850	0.863	0.316	0.602
l/A (cm^{-1})	11.04	9.86	22.7	13.35
q	−0.043 76	−0.022 35	−0.065 89	−0.033 87
r	−0.527 8	−0.706 1	−0.544 7	−0.710 5
s	3.815	4.025	3.960	4.166
h_m (eV) 298 K	0.16	0.17	0.20	0.19
h_m (eV) 473 K	0.14	0.16	0.16	0.17

(Not all the crystals were measured to the lowest temperature.) After the first set was completed, there appeared to be inconsistency in the results; they indicated substantial rotation of the σ_1 and σ_3 principal axes as a function of temperature. Such rotation is not precluded for the properties of monoclinic crystals. However, it has been demonstrated[8] that the electrical conductivities of the halogenide solid electrolytes are so intimately related to their crystal structures as to make such rotation unlikely for α-$Ag_{26}I_{18}W_4O_{16}$. The inconsistency of the results for the α phase was attributed to one or more of the following: poor electrode contact, poor crystal quality, insufficient length to area ratio. These did not affect the observations of the transition temperatures. All four crystals gave 246 K for the α-β transition, and three of the four gave 197 K for the β-γ transition; the fourth gave 198 K for this transition. Figure 2 shows these transitions obtained from measurements of crystals in the $\vec{a}$ and $\vec{c}^*$ directions. The l/A ratios for these crystals are 5.1 and 3.9 cm^{-1}, respectively. There appeared to be little hysteresis in the transitions for these crystals as compared with that shown by the results of measurements on crystals with much larger l/A ratios (see Fig. 3).

In the second set of measurements, greater care was taken in the selection of crystals, in the preparation of the silver electrodes put onto the crystals as described earlier, and the l/A ratios[9] (Table I) were substantially increased. Crystals taken through the second transition developed cracks. This did not occur through the first transition, indicating perhaps that the α-β transition represents a smaller change than the β-γ transition.

Results of the second set of measurements are plotted[10] as $\log_{10}\sigma T$ vs $10^3/T$ in Fig. 3. It will be noticed that for the α phase, none of these plots is a straight line (see Discussion). Parabolic fits of the form

$$\log_{10}(\sigma T) = qx^2 + rx + s\,, \quad x = 10^3/T \qquad (5)$$

were made to the data. The results are shown in Table I. Shown in Table II are some values of σ, obtained from the fitted curves for some specific values of temperature, compared with actual observed values. For the most part the fits are very good, i.e., to better than 1%.

Values of σ_{13} were calculated from (2) with values of σ_{ii} and $\sigma_{\vec{c}}$ obtained from the parabolic relations at 25° intervals from −25° to 200°C. Also the magnitudes of the conductivities along the principal axes were calculated. Results are shown in Table III. Included are the rotation angles calculated from (4). These angles give a smooth curve when plotted as radians vs T except for the point at 200°C. At first glance, the rotation appears to

TABLE II. Values of $\sigma_{ii}T$ and $\sigma_{\vec{c}}$ at 25° increments of temperature. For each temperature, results on the first line are from parabolic fits, on the second line either from direct measurements or read from graphs.

$(T-0.15)$ (K)	10^3T^{-1} (K^{-1})	$\sigma_{11}T$	$\sigma_{22}T$	$\sigma_{33}T$	$\sigma_{\vec{c}}T$
		(Ω^{-1} cm^{-1} K)			
273	3.661	19.8	13.8	12.1	12.9
		19.8	14.0	12.1	13.0
298	3.354	35.7	25.4	24.7	25.2
		35.2	24.0	24.8	24.6
323	3.095	57.8	42.2	44.0	43.9
		57.7	42.3	44.2	44.3
348	2.872	86.7	64.9	71.1	70.1
		87.2	65.5	70.0	70.3
373	2.680	122.0	93.7	106.4	104.3
		123.1	95.0	107.6	102.8
398	2.512	163.3	128.9	150.0	147.0
		164.4	130.3	151.0	148.7
423	2.363	210.6	170.4	201.8	198.5
		210.9	170.1	199.8	199.0
448	2.231	262.8	217.9	261.1	258.3
		262.2	216.3	261.9	257.6
473	2.114	318.9	270.6	326.6	325.5
		316.6	267.7	323.9	323.8

TABLE III. Values of conductivities (Ω^{-1} cm^{-1}) at 25° increments of temperature obtained from the parabolic fits in columns 2–5, all values in subsequent columns calculated from these (see text). Experimental error permits the assumption that the σ_{ii} in columns 2–4 are the principal conductivities.

$(T-0.15)$ (K)	σ_{11}	σ_{22}	σ_{33}	$\sigma_{\vec{c}}$	σ_{13}	θ (rad)	$\langle\sigma\rangle$	σ_1'	σ_3'
273	0.0724	0.0506	0.0443	0.0472	−0.0027	−0.095	0.0558	0.0727	0.0440
298	0.120	0.0853	0.0826	0.0846	−0.0005	−0.007	0.0966	0.120	0.0826
323	0.179	0.131	0.136	0.136	0.0053	0.061	0.149	0.180	0.135
348	0.249	0.187	0.204	0.201	0.012	0.13	0.213	0.252	0.201
373	0.327	0.251	0.285	0.280	0.016	0.18	0.288	0.332	0.280
398	0.410	0.324	0.377	0.370	0.019	0.26	0.370	0.419	0.368
423	0.497	0.403	0.477	0.469	0.019	0.38	0.459	0.508	0.466
448	0.586	0.486	0.582	0.576	0.013	0.64	0.551	0.597	0.571
473	0.675	0.572	0.691	0.689	0.002	−0.12	0.646	0.675	0.691

be substantial. However, it turns out in *every* case that a one percent or less change in the parameters that enter (4), appropriately chosen, reduce these angles to zero. The substantial sensitivity of the rotation angle to small errors in measurement is combined with an insensitivity of the changes in magnitude in the diagonal terms of the tensor to the principal axis values (labeled σ_1' and σ_3' in Table III). Thus while it is very likely that the principal conductivity axes in the monoclinic plane are always along $\vec{a}$ and $\vec{c}^*$ in the α phase, it is not a certainty.

The $\log_{10}(\sigma T)$ vs T^{-1} plots for the β and γ phases fit very well to straight lines. The slopes give values of the enthalpies of activation of motion for the β phase as follows: 0.25, 0.25, 0.32, and 0.33 eV along $\vec{a}$, $\vec{b}$, $\vec{c}^*$, and $\vec{c}$ respectively, and for the γ phase 0.65, 0.46, 0.53, and 0.55 eV along $\vec{a}$, $\vec{b}$, $\vec{c}^*$, and $\vec{c}$, respectively.

Corrections for thermal expansion have not been made. In the cases of the β and γ phases, we do not know what the conductivities represent relative to their conductivity tensors anyway. No low-temperature x-ray diffraction work has been done as yet. As to the α phase, the photograph taken at 150°C indicates an approximately one-percent increase in magnitude of a and c relative to the 25°C values. This implies somewhat less than a two-percent increase at 200°C. The conductivities are obtained from $\sigma = l/AR$ where R is the measured resistance. Therefore, errors in the values of σT from omission of corrections for thermal expansion are at most less than two percent, and the curvature of the $\log_{10}(\sigma T)$ vs T^{-1} curves would actually be decreased slightly if the corrections were made.

Equation (1) is actually a general equation for finding the conductivity in any direction in a crystal if the tensor components are known. The average conductivity is therefore

$$\langle\sigma\rangle = \sum_{i,j=1}^{3} \sigma_{ij}\langle l_i l_j\rangle. \tag{6}$$

This gives the result that for any crystal

$$\langle\sigma\rangle = \Big(\sum_{i=1}^{3} \sigma_{ii}\Big)\Big/3\,; \tag{7}$$

that is, for any crystal $\sum\sigma_{ii}$ $(=\sum\sigma_i)$ is invariant. (Here σ_i designate the principal axis conductivities.)

The values of Table III have been used for the plot of $\log_{10}(\langle\sigma\rangle T)$ vs T^{-1} in Fig. 4. The curve is expressible by the parabola

$$\log_{10}(\langle\sigma\rangle T) = -0.037\,44x^2 - 0.6255x + 3.975\,,$$
$$x = 10^3/T.$$

The values of h_m, the enthalpy of activation of motion, are 0.17 and 0.16 eV at 25 and 200°C, respectively (see Discussion).

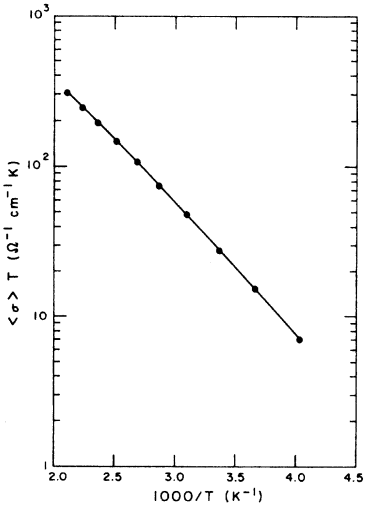

FIG. 4. Plot of $\log_{10}$ of the average conductivity multiplied by temperature vs reciprocal temperature.

DISCUSSION

Considerable emphasis has been given the results that for the α phase, the plots of $\log_{10}(\sigma T)$ vs T^{-1} are nonlinear and can be fitted quite well with parabolas. It has already been shown above that omission of corrections for expansion does not account for this curvature. There does not seem to be any reason to suppose that the small change in the β angle with increasing temperature should in itself relate to this curvature.

We can write the relation for the conductivities of the anisotropic, solid electrolyte containing Ag^+ ions:

$$\sigma_i = ne\mu_i, \quad i = 1, 2, 3 \tag{8}$$

in which the subscript i refers to the ith principal conductivity axis, n to the carrier concentration, and μ_i to the mobility in the x_i direction. It should be emphasized that even for an isotropic conductor like α-$RbAg_4I_5$, μ_i is an average mobility because the barriers and potential wells are not all crystallographically equivalent.

The theory of diffusion in solids is highly simplified, especially relative to $Ag_{26}I_{18}W_4O_{16}$. However, it appears that it should contain the essence of the parameters involved in the relation for the conductivity when the Nernst-Einstein relation is used.[11] If the number of mobile cations is constant, one still needs a correlation factor or Haven ratio,[12] f, which depends largely on the crystal structure. This factor might well be included as a parameter *in* n. The factor reduces the total number of mobile cations mainly as a result of cation-cation interaction. That is, there are constraints on the movements of the charge carriers (see e.g., Refs. 8, 13–15).

Because the original theoretical work assumes isotropic diffusion, f is not considered to be anisotropic. However, in an anisotropic solid, f will be anisotropic. If it is taken to be part of n in the expression for the conductivities, then we should have

$$\sigma_i = n_i e\mu_i, \quad i = 1, 2, 3 \tag{9}$$

in which again, i refers to the principal axis. Also h_m must be considered to be anisotropic; in fact, as indicated earlier, even in each direction, it is an average value. For simplicity, however, the values of n and h_m will not be subscripted in the following discussion.

Now in the case of $Ag_{26}I_{18}W_4O_{16}$, it has been shown[1] that at room temperature, more than half the Ag^+ ions are probably not mobile. It is possible that when the temperature is increased some Ag^+ ions from the "bypass" sites are excited into the mobile category. *Qualitatively*, the intensities on the photographs (mentioned earlier) taken at 110 and 150°C do not indicate any drastic change as contrasted with the case of $(C_5H_5NH)Ag_5I_6$ (Ref. 14).

The mobility contains a Boltzmann factor $\exp(-h_m/kT)$ and if we are to accept the possibility that n is not constant in $Ag_{26}I_{18}W_4O_{16}$, it should also contain a Boltzmann factor. However, it must be recognized that there is a temperature-independent concentration of mobile charge carriers, so that the factor should look like[16] $[1+\exp(-h_f/2kT)]$. We then have that

$$\sigma T = C[1+\exp(-h_f/2kT)]\exp(-h_m/kT), \tag{10}$$

in which C contains a number of parameters essentially independent of temperature. The slope

$$d\ln(\sigma T)/d(T^{-1}) = -\{h_m + h_f/2[1+\exp(h_f/2kT)]\}/k, \tag{11}$$

from which it is seen that as the temperature is increased, a contribution from the promotion of silver ions from the "bypass" sites into the mobile category should increase the steepness of the slope. Thus, this is not the source of the downward concavity with increase in temperature.

It appears that there is only one remaining possibility, namely that for the α phase, the enthalpies of activation of motion of the charge carriers are temperature dependent with the possible form $h_m = 2qx + r$ ($x \equiv 1000/T$). This is an empirical conclusion resulting from the parabolic fits to the observed data [see Eq. (5)].

Because of the experimental error discussed earlier, we suggest tentatively that the principal axes are along $\vec{a}$, $\vec{b}$, and $\vec{c}^*$. Therefore we can set σ_{ii} of the second, third, and fourth columns of Table III equal to σ_i which refer to the principal axis components of the conductivity tensor. Because the structure of α-$Ag_{26}I_{18}W_4O_{16}$ is complex, all that can be said about the magnitudes of the σ_i is that they are compatible with the structure at room temperature. Table III shows that σ_2 decreases from a value slightly greater than that of σ_3 to the lowest value at 473 K. Also σ_1 decreases from a value more than 1.5 times that of σ_3 to a value smaller than that of σ_3 at 473 K. Both these are anticipated by the relative slopes of $\log_{10}\sigma T$ vs T^{-1}.

At first glance, an argument that a lower conductivity may imply "easier" conduction appears to be contradictory. However, "easier" conduction is implied by lower h_m (see for example, Ref. 17) and the structure suggests that the "hardest" conduction direction is $\vec{c}^*$ because of the "walls" described in Ref. 1. This is the direction of highest h_m. In any case, the differences in h_m are not

really large (Table I).

It should be noted that the conductivities shown in Table III are substantial. Furthermore, the parabolic equations predict values of 1.01, 0.93, 1.12, and 1.02 Ω^{-1} cm^{-1} for σ_1, σ_2, σ_3, and $\langle\sigma\rangle$, respectively, at 300°C which is just below the melting point.

The plot of $\log_{10}\langle\sigma\rangle T$ vs T^{-1} still shows a slight concavity, which is not shown by the original plot based on polycrystalline material. The values of h_m range from 0.17 eV at 25° to 0.16 eV at 200°C. These values are not far from the value 0.18 eV found from the measurements on the polycrystalline material.[1] However, the values of $\langle\sigma\rangle$ obtained from measurements on the single crystals are substantially higher than those obtained from the polycrystalline material. At 25°C, the ratio is 1.6. We can only infer from the deviation of the bulk density of the polycrystalline specimen from the x-ray density by only 4% (see Ref. 1) that particle contact was insufficient to give accurate values of the conductivity.

Although an x-ray diffraction investigation of the low-temperature phases has not been done, we offer some speculations on their nature. First, the h_m values are rather high for the β phase and very high for the γ phase. This implies increased order of the Ag^+ ions in the β phase and possibly, but not necessarily, complete order in the γ phase.

If a compound or element has more than one crystal structure, it is usual (but not always) that the high-temperature structure has a higher symmetry, and also it happens often that the lower-symmetry structures have larger primitive cells. If the β phase has lower symmetry than the α phase, it must belong to the lowest-symmetry point group 1 (C_1) and therefore the lowest symmetry space group $P1$ (C_1^1). In such a case, the symmetry of the $(W_4O_{16})^{8-}$ entity would be reduced to identity symmetry and the unit cell would be closely related to the primitive cell of the α phase. The γ phase is also very likely triclinic with a larger cell than that of the β phase.

ACKNOWLEDGMENT

This work was supported by the National Science Foundation under Grant No. DMR-11378-A01.

---

*Present address: Storage Technology Corporation, 2270 South 88 Street, Louisville, Colorado 80027.

†Present address: Union Carbide Corp., Parma Research Center, Parma, Ohio 44130.

‡Present address: Institut "Josef Stefan," Jamova 39, 61001 Ljubljana, Yugoslavia.

[1]L. Y. Y. Chan and S. Geller, J. Solid State Chem. 21, 331 (1977).

[2]A. Imai and M. Harata, J. Electrochem. Soc. 117, 117 (1970); M. S. Whittingham and R. A. Huggins, J. Chem. Phys. 54, 414 (1971).

[3]T. Hibma, Phys. Rev. B 15, 5797 (1977).

[4]T. Takahashi, S. Ikeda, and O. Yamamoto, J. Electrochem. Soc. 120, 647 (1973). The indication that the solid electrolyte melted incongruently was correct, even though the authors reported an incorrect formula for the solid electrolyte (see Ref. 1).

[5]S. Geller, J. R. Akridge, and S. A. Wilber, Phys. Rev. B 19, 5396 (1979).

[6]J. E. Bauerle, J. Phys. Chem. Solids 30, 2657 (1969).

[7]J. F. Nye, *Physical Properties of Crystals* (Oxford University Press, London, 1972).

[8]S. Geller, in *Solid Electrolytes*, edited by S. Geller (Springer, Heidelberg, 1977), pp. 41–64, and pertinent references therein.

[9]The cross-sectional areas of the crystals were irregular. Therefore the area of each crystal was determined from $A = m/\rho l$, where m is the mass, l the length, and ρ the x-ray density.

[10]The plot for the c axis direction is omitted because it overlaps almost exactly that for the $\vec{c}^*$ direction. (See also Tables II and III.)

[11]See for example, H. Wiedersich and S. Geller, in *The Chemistry of Extended Defects in Non-Metallic Solids*, edited by L. Eyring and M. O'Keeffe (North-Holland, Amsterdam, 1970), pp. 629–650.

[12]Y. Haven, in *Fast Ion Transport in Solids*, edited by W. van Gool (North Holland/American Elsevier, Amsterdam/New York, 1973), pp. 35–49.

[13]S. Geller, Phys. Rev. B 14, 4345 (1976).

[14]S. Geller and B. B. Owens, J. Phys. Chem. Solids 33, 1241 (1972).

[15]L. Y. Y. Chan, S. Geller, and P. M. Skarstad, J. Solid State Chem. 25, 85 (1978).

[16]For the factor $\exp(-h_f/2kT)$ where h_f is the enthalpy of formation of a defect, see for example, P. W. M. Jacobs and F. C. Tompkins, Q. Rev. Chem. Soc. London 6, 238 (1952). Also see R. D. Armstrong, R. S. Bulmer, and T. Dickinson, J. Solid State Chem. 8, 219 (1973).

[17]H. Sato, in *Solid Electrolytes*, edited by S. Geller (Springer, Heidelberg, 1977), pp. 3–39.